



Published in final edited form as:

J Orthop Res. 2011 June ; 29(6): 931–937. doi:10.1002/jor.21342.

Cryoinsult Parameter Effects on the Histologically-Apparent Volume of Experimentally-Induced Osteonecrotic Lesions

Jessica E Goetz^{+,§}, Duane A Robinson^{*}, Douglas R Pedersen^{+,§}, Michael G Conzemius^{*}, and Thomas D Brown^{+,§}

⁺Department of Orthopaedics & Rehabilitation, University of Iowa, Iowa City, IA

[§]Biomedical Engineering, University of Iowa, Iowa City, IA

^{*}College of Veterinary Medicine, University of Minnesota, St. Paul, MN

Abstract

Investigation of femoral head osteonecrosis would benefit from an animal model whose natural history includes progression to bony collapse of a segmental necrotic lesion. The bipedal emu holds attraction for systematic organ-level study of collapse mechanopathology. One established method of experimentally inducing segmental lesions is liquid nitrogen cryoinsult. Four cryoinsult parameters – hold temperature, freeze duration, freeze/thaw repetition, and thaw duration - were investigated to determine their individual and combined effects on resulting necrotic lesion morphology. 3D distributions of histologically-apparent osteocyte necrosis from 24 emus receiving varying cryoinsults were used to develop univariate and multivariate linear regression models relating resulting necrotic lesion morphology to particular cryoinsult input parameters. These models were then applied to predict lesion size in four additional emus receiving differing input cryoinsults. The best multivariate regression model predicted lesion volumes that were accurate to better than 8% of overall emu femoral head volume. The hold temperature during cryoinsult was by far the most influential cryoinsult input parameter. The utility of this information is to enhance the consistency and predictability of cryoinsult-induced segmental lesion size for the purposes of systematic laboratory studies at the whole-organ level.

Keywords

Femoral Head Osteonecrosis; Cryoinsult; Linear Regression; Emu

Introduction

The watershed clinical event in femoral head osteonecrosis (ON) is bony collapse of the normally spherical femoral head as a result of structural compromise within a localized bone infarction. Since clinical presentations vary so widely (e.g., lesion size/location and etiology), systematic investigation of treatment and prevention strategies is best performed in animal models in which consistent osteonecrotic lesions are artificially induced. The bipedal emu appears to be a useful model of ON due to its development of human-like microscopic ON pathology and its progression to human-like necrotic femoral head collapse.¹ One established method^{1,2} for creating experimental necrotic lesions is liquid nitrogen cryoinsult. Although artificial, this insult modality is more effective for creating a focal lesion than clinically-encountered induction methods, such as systemic steroids.³

Experimenter-controlled cryoinsult parameters include hold temperature, freeze duration, thaw duration, and freeze/thaw repetition. Presumably, differing combinations of parameters would result in cryoinsults of different severities, therefore creating different volumes of necrotic tissue.

The effects of individual and specific combinations of cryoinsult parameters on soft tissue ablation have been extensively investigated, both at the cellular and at the tissue levels. Investigations of breast, renal, and prostate cancer cell lines demonstrated increased cell death with colder temperatures, with additional freeze cycles, or with longer freeze duration.⁴⁻⁶ Studies of intact soft tissues (liver, skin, kidney) showed similar results, with the added finding that slow thaw time increased cell death.⁷⁻¹⁰ However, reports on the effects of specific cryoinsult parameters have sometimes been conflicting. For example, Woolley et al.¹¹ found that thaw rate had a minimal impact on the amount of ablated renal tissue, whereas Neel and DeSanto¹² found that the thaw rate was an important parameter affecting tumor tissue viability.

Effects of cryoinsult parameter sets on tissue viability vary by tissue type. In a study using an identical set of cryoinsult parameters in kidney, liver, and lung tissue, the ablation region extended 21 mm, 8 mm, and 12 mm away from the cryoprobe center, respectively.¹³ Because the effects of cryoinsult parameters are so tissue specific, cryoinsult-induced segmental lesion creation in cancellous bone cannot be predicted from soft tissue experience. To determine the specific effects of cryoinsult parameters on emu cancellous bone, for the purposes of establishing control over the size of osteonecrotic lesions induced during a surgical cryoinsult procedure, a parametric series of intraoperative cryoinsults was performed. The necrotic lesion resulting from each cryoinsult was evaluated using a novel 3D histology method. Univariate and multivariate linear regression models were developed to explore the effects of individual and specific combinations of cryoinsult parameters on the morphology of the induced necrotic lesion.

Methods

3D Histological Evaluation

In an IACUC-approved procedure, 28 emus received a cryoinsult to the right femoral head by means of a cryoprobe^{14,15} inserted through a lateral surgical approach. The animals were divided into 5 different cryoinsult groups. 24 animals divided into 4 groups (Groups 1-4) comprised a teaching set, which was used to determine the effects of individual cryoinsult input parameters on lesion size (Table 1). The remaining 4 animals comprised a testing set (Group 5), which was used to evaluate the predictive ability of regression models developed from the teaching set data, to estimate the effects of cryoinsult input parameters on resulting necrotic lesion size.

One week after surgical cryoinsult, the animals were euthanized, and the proximal third of the operated femur was harvested and fixed in formalin. Using a custom alignment fixture, each femur was potted vertically in PMMA to establish registration. A guide was used to drill two parallel AP-directed fiducial holes (10 mm apart, 1.6 mm in diameter) through the femoral neck. The femoral head was then separated from the proximal femur by two orthogonal saw cuts made lateral and distal to the fiducial drill holes. The fiducial holes afforded registration of subsequent histology sections. To prevent distortion of the relatively small fiducial holes in the coarsely trabeculated emu cancellous bone during histological processing, two dowels of partially dehydrated potato were inserted into the holes after decalcification to serve as fiducial markers. Specimens were then embedded in paraffin and serially sectioned through the entire head in the coronal plane, perpendicular to the fiducial

markers. 5-micron sections selected at 1-mm intervals through the entire head were stained with Weigert's hematoxylin and eosin.

Slides were digitized in grayscale on a stepper-motor-driven microscope stage (StagePro, Prior Scientific, Rockland MA), resulting in ~2200 tif files of tissue sub-regions per section, each 0.485×0.637 mm (Fig. 1). Every tissue sub-region that included mineralized bone was evaluated for osteocyte viability (percentage of nuclei-filled lacunae) using a custom-written Matlab (MathWorks, Natick, MA) program.^{3,15} Sub-regions that were empty of mineralized bone (e.g. marrow space or drill tract) were marked as vacant. Once all sub-region images comprising a given histological section were evaluated, the resulting 2D data array mapped osteocyte viability over the entire histology section. Per the criterion of Koo et al., a sub-region was defined as necrotic if <50% of its osteocytes were viable.¹⁶ Adjacent viability maps from a given femoral head were rotated and translated so as to align the fiducials on each section, and thereby register the planar viability data in the 3rd dimension (Fig. 2).

For consistency of subsequent lesion geometry calculations, a drill tract-based coordinate system was adopted. Within the necrotic region in each 2D histology section, the coordinates of the largest patch of sub-region images that had been categorized as vacant indicated the drill tract. The z-axis for the tract-based coordinate system was defined by a principal component analysis straight-line fit to those drill tract centroids in 3D space. The lesion was nominally axisymmetric as a result of being induced by a cylindrical probe, so the other principal axes of the lesion were not readily identifiable. Therefore, the lesion x-axis was defined by vectorially crossing the lesion z-axis with the global x-axis (horizontal direction in the plane of histological sectioning), and the lesion y-axis was defined by crossing the lesion z-axis with the lesion x-axis. This tract-based coordinate system was centered at the (leading) tip of the drill tract (Fig. 2).

Next, a smoothed lesion surface was defined by fitting a series of circles to the lesion boundary at 1-mm increments along the z-axis. The volume enclosed by this smoothed lesion surface was calculated by numerical integration. Lesion volumes were restricted to include only the necrotic bone distal to the tip of the cryoprobe, plus the necrotic volume along the distal-most 13 mm of the drill tract. This avoided including bone that had been collaterally damaged by the drilling operation prior to cryoprobe insertion. The percentage of the femoral head involved in each lesion was then calculated by dividing lesion volume by the volume of an average emu head (approximated as a 25-mm diameter sphere). Maximum lesion radius and the length of lesion extension past the end of the drill tract were also recorded. These four outcome variables (two volumetric and two linear) were associated with the particular set of cryoinsult parameters that had been used to create the lesion.

Regression Analysis of Cryoinsult Parameters

To model the effects of each *individual* cryoinsult parameter on lesion morphology, linear regression was performed on the outcome variables from each of the four teaching groups. Each such univariate linear regression model used as its input either cryoinsult hold temperature, freeze duration, number of freeze/thaw cycles, or thaw duration, and reported as its output either histologically-measured lesion volume (in mm³), percent femoral head involvement, maximum lesion radius (in mm), or lesion extension past the end of the drill tract (in mm).

To estimate the lesion morphology that would be generated by a given *combination* of cryoinsult parameters, multivariate linear regression models using all four cryoinsult input variables were also fit to the outcome data variables. Additionally, the *Best Subsets* option in Minitab 15 (Minitab Inc. State College, PA) was used to screen additional multiple

regression models that used fewer input parameters in different combinations. This was intended to eliminate the effects of overfitting¹⁷ and identify the simplest feasible model.¹⁸ The best one-, two-, and three-input regression models were selected based on the adjusted R^2 value (larger being a better fit), the standard error (smaller being a better fit), and the Mallows' C_p value (closer to the number of variables in the model being a better fit).¹⁹ All regression models were initially (internally) validated on the teaching set to verify performance, and then were applied to the data from Group 5 (the testing set) to estimate the predictive ability of the respective models.

Results

Approximately 20 2D serial histology sections were analyzed per emu femoral head. Analysis of each head required ~25-30 hours for scanning and ~30 hours for osteocyte viability grading and 3D reconstruction. The osteonecrotic lesions created in the parametric study occupied 3% to 20% (Fig. 3) of the femoral head volume, and maximum lesion radii ranged from 3 to 6.9 mm (Fig. 4). The necrotic lesions extended as far as 7.4 mm past the tip of the drill tract.

Linear regression performed on the individual cryoinsult groups revealed varying effect sizes. Necrotic lesion volume increased significantly and nearly linearly with a decrease in cryoinsult hold temperature. Increasing the number of freeze/thaw repetitions slightly increased lesion volume. However, lesion volumes increased only minimally with longer freeze or thaw durations. Comparisons of R^2 values and the regression equation slopes across all four groups indicated that the cryoinsult hold temperature was by far the most dominant cryoinsult parameter affecting lesion size (Figs. 3 & 4). The low R^2 values calculated for cryoinsult freeze/thaw repetition, and especially for freeze duration and thaw time, indicated minimal association between these cryoinsult parameters and lesion volume (over the parameter space investigated).

The four-input multivariate linear regression model best describing lesion volume was: $Volume = -292 - 25.3*Temp + 72.9*Cycles + 27.5*Time_{Freeze} + 7.4*Time_{Thaw}$, where volume is expressed in mm^3 , temperature is expressed in $^{\circ}C$, cycles is expressed as the number of freeze/thaw repetitions, and time is expressed in minutes. Only the coefficient in this equation associated with the temperature input variable was significant ($p < 0.05$). The lack of significance of the coefficients associated with the other inputs indicated that these variables did not detectably influence the model's ability to predict lesion volume. The similarity in temperature coefficients in the four-input (-25.3) and single-input (-25.8) regression models indicated that the additional cryoinsult input parameters made small contributions to lesion volume prediction beyond what was predictable by hold temperature alone.

Because using all of the input parameters did not improve the predictive ability of the regression model over what was achievable with hold temperature alone, models with fewer of these non-contributing variables merited exploration. The best one-, two-, and three-variable models identified using the *Best Subsets* function in Minitab were:

$$Volume = 190 - 25.8 * Temp$$

$$Volume = 123 - 24.2 * Temp + 23.5 * Time_{Thaw}$$

$$Volume = -324 - 25.8 * Temp + 86.6 * Cycles + 28.9 * Time_{Freeze}$$

These reduced-input regression models and the full four-input regression model were run on the 24 specimens from the teaching set (Groups 1-4) to determine the quality of each model in terms of its ability to accurately fit the lesion volumes. The four different lesion volumes

estimated for each specimen by the different regression models were similar to each other, typically differing by <10% of the specimen's histologically measured lesion volume.

Agreement between the regression-inferred versus the histologically-determined lesion volumes was expressed both as a percentage of the histologically measured lesion volume, and as a percentage of overall emu femoral head volume. All four regression models were able to predict lesion volumes to within $\pm 25\%$ of the histologically measured lesion volume in 16 of 24 heads with no specific trend for over- versus under-estimation of lesion size. Errors in regression-estimated lesion volumes corresponded to 0.1% to 5.9% of the femoral head volume, a small enough bone fraction to seemingly have little influence on the propensity for necrotic femoral head collapse.

The multivariate regression models were then used to estimate lesion volumes for the four femoral heads in Group 5 (Fig. 5). The full four-input model estimated lesion volumes were accurate to within 25 to 35% of the histologically measured lesion volume (average 30% error), which corresponded to 1 to 7% of total femoral head volume. Again, there was no specific trend for over- versus under-estimation of lesion size. Because the reduced-input regression models were not confounded by overfitting experimental noise, they were slightly more accurate in predicting lesion volumes. Specifically, the regression model using hold temperature and thaw time performed best in terms of estimating lesion volumes in Group 5. This particular model estimated lesion volumes accurate to within 8 to 32% of measured histologically-measured lesion volume (average 20% error), which, depending on the size of the lesion, corresponded to an error of 1 to 8% of total femoral head volume.

Discussion

For purposes of a well-controlled animal model of femoral head ON, the ability to systematically modulate segmental lesion morphology is critical. The amount of osteonecrotic tissue generated by a given cryoinsult was histologically evaluated based on the cryoinsult parameters of cryoinsult hold temperature, freeze duration, number of freeze/thaw cycle repetitions, and thaw duration. Effects of changes to these parameters were fit by linear regression models. Both single and multivariate regression analyses indicated that cryoinsult hold temperature was by far the most influential input parameter in terms of altering the morphology of the resulting necrotic lesion.

Hold temperature is a factor that intuitively would have substantial impact on the volume of the necrotic lesion created. The small changes in lesion volume resulting from changes in the other three cryoinsult parameters may have been a product of the smaller influence of these factors on cell death, or of the fairly narrow parameter ranges that were investigated, or perhaps both. However, the individual insult parameter ranges needed to be restricted to what was practical experimentally,¹ especially in terms of intra-operative time and anesthesia duration. In the soft tissue cryoablation, additional freeze time or thaw time and additional cycles of repetition increase the fraction of dead cells within a frozen region, without appreciably increasing the geometric size of that frozen region.^{10,11,20} Considering that evidence, it is plausible that the effects of the freeze and thaw duration on the lesion volume were not fully apparent in our work because only the region of <50% osteocyte viability was considered. Had the volumes of 25% or 0% osteocyte viability been studied, freeze/thaw duration or repetition might have demonstrated more of an effect. However, the <50% criterion of Koo et al.¹⁶ is the most widely accepted histological criterion for osteonecrosis, and therefore it was the definition used in this work.

The cryoinsult parameter sets used in the testing set (Group 5) included different parameter combinations than those used in the teaching groups. Applying the same multivariate

regression models to cryoinsults consisting of different parameter combinations necessarily assumed identical effects of each input variable, independent of changes to the other variables. This assumption appeared to be reasonably valid because the multivariate linear regression models were capable of estimating accurate lesion volumes (mean error of 20% of histologically-measured volume), even for those specimens with cryoinsult parameter sets that were not included in any of the teaching groups. The errors involved represented clinically negligible amounts of bone (1-8% of emu femoral head volume).

Inclusion of more specimens in the teaching set, for purposes of being able to fit the regression models to more data points, might have helped improve determination of the contributions from cryoinsult parameters other than the hold temperature. It was clear, however, that the effects of hold temperature were greatly predominant, so having higher significance for the “small effect” cryoinsult parameters had to be balanced against animal usage and analysis time required per specimen. While analysis time could have been substantially reduced by organ-level MR imaging, correlations between MRI signal and actual tissue-level pathology remain controversial, even for the well-investigated situation of human clinical cases.²¹⁻²³

Another limitation to this work relates to the cryoinsult surgery itself. In a few instances, due to cryoprobe placement (ideally juxta-articularly within the main weightbearing tract), the region of necrosis extended slightly outside the bony tissue available for analysis (i.e. into the cartilage). Because of this factor, some of the volumes measured with the 3D histology method may have been artifactually low. These instances of volume underestimation would have had the greatest influence on conclusions made when exploring the cryoinsult parameters individually, because of a smaller number of data points (5-10) used to develop the univariate regression models. By developing the multivariate regression models from all of the lesions, the higher number of data points (24) served to moderate potential bias associated with these occasional low-volume measurements.

Linear regression models were able to reasonably correlate the histologically measured lesion volume data with the four cryoinsult input parameters. From these models, the hold temperature at the cryoprobe tip was the predominant parameter influencing the volume of necrotic cancellous bone. Similar to existing reports in the cryoablation literature, freeze duration, number of freeze/thaw cycle repetitions, and thaw duration had a much smaller influence on tissue viability. Therefore, when choosing a parameter set to produce an experimental necrotic lesion of a particular size in (emu) cancellous bone, it would be most effective simply to control the cryoinsult hold temperature, rather than to perform complex and lengthy cryoinsult procedures involving multiple repetitions of intricately-timed freeze/thaw cycles.

Acknowledgments

This work was funded by National Institutes of Health grant AR049919.

References

1. Conzemi MG, Brown TD, Zhang Y, Robinson RA. A new animal model of femoral head osteonecrosis: one that progresses to human-like mechanical failure. *J Orthop Res.* 2002; 20:303–9. [PubMed: 11918310]
2. Bowers JR, Dailiana ZH, McCarthy EF, Urbaniak JR. Drug therapy increases bone density in osteonecrosis of the femoral head in canines. *J Surg Orthop Adv.* 2004; 13:210–6. [PubMed: 15691182]

3. Goetz JE, Chung YY, Zimmerman DL, Pedersen DR, Robinson DA, Conzemius M, Brown TD. Steroid-induced versus cryoinsult-induced femoral head osteonecrosis: Statistical measurement of histologic abnormality focalization. *J Musculoskeletal Res.* 2005; 9:161–72.
4. Clarke DM, Robilotto AT, Rhee E, VanBuskirk RG, Baust JG, Gage AA, Baust JM. Cryoablation of renal cancer: variables involved in freezing-induced cell death. *Technol Cancer Res Treat.* 2007; 6:69–79. [PubMed: 17375969]
5. Klossner DP, Robilotto AT, Clarke DM, Vanbuskirk RG, Baust JM, Gage AA, Baust JG. Cryosurgical technique: Assessment of the fundamental variables using human prostate cancer model systems. *Cryobiology.* 2007; 55:189–99. [PubMed: 17888898]
6. Rui J, Tatsutani KN, Dahiya R, Rubinsky B. Effect of thermal variables on human breast cancer in cryosurgery. *Breast Cancer Res Treat.* 1999; 53:185–92. [PubMed: 10326796]
7. Auge BK, Santa-Cruz RW, Polascik TJ. Effect of freeze time during renal cryoablation: a swine model. *Journal of Endourol.* 2006; 20:1101–5.
8. Gage AA, Guest K, Montes M, Caruana JA, Whalen DA Jr. Effect of varying freezing and thawing rates in experimental cryosurgery. *Cryobiology.* 1985; 22:175–82. [PubMed: 3979086]
9. Gill W, Fraser J, Carter DC. Repeated freeze-thaw cycles in cryosurgery. *Nature.* 1968; 219:410–3. [PubMed: 5662164]
10. Larson TR, Robertson DW, Corica A, Bostwick DG. In vivo interstitial temperature mapping of the human prostate during cryosurgery with correlation to histopathologic outcomes. *Urology.* 2000; 55:547–52. [PubMed: 10736499]
11. Woolley ML, Schulsinger DA, Durand DB, Zeltser IS, Waltzer WC. Effect of freezing parameters (freeze cycle and thaw process) on tissue destruction following renal cryoablation. *J Endourol.* 2002; 16:519–22. [PubMed: 12396446]
12. Neel HB 3rd, DeSanto LW. Cryosurgical control of cancer: effects of freeze rates, tumor temperatures, and ischemia. *Ann Otol Rhinol Laryngol.* 1973; 82:716–23. [PubMed: 4743401]
13. Permpongkosol S, Nicol TL, Link RE, Varkarakis I, Khurana H, Zhai QJ, Kavoussi LR, Solomon SB. Differences in ablation size in porcine kidney, liver, and lung after cryoablation using the same ablation protocol. *AJR Am J Roentgenol.* 2007; 188:1028–32. [PubMed: 17377040]
14. Reed KL, Brown TD, Conzemius MG. Focal cryogen insults for inducing segmental osteonecrosis: Computational and experimental assessments of thermal fields. *J Biomech.* 2003; 36:1317–26. [PubMed: 12893040]
15. Goetz JE, Pedersen DR, Robinson DA, Conzemius MG, Baer TE, Brown TD. The apparent critical isotherm for cryoinsult-induced osteonecrotic lesions in emu femoral heads. *J Biomech.* 2008; 41:2197–205. [PubMed: 18561937]
16. Koo KH, Jeong ST, Jones JP Jr. Borderline necrosis of the femoral head. *Clin Orthop Relat Res.* 1999; 358:158–65. [PubMed: 9973987]
17. Hawkins DM. The problem of overfitting. *J Chem Inf Comput Sci.* 2004; 44:1–12. [PubMed: 14741005]
18. Katz, MH. *Multivariable analysis: Practical guide for clinicians.* 2nd. New York: Cambridge University Press; 2006.
19. Hocking RR. The analysis and selection of variables in linear regression. *Biometrics.* 1976; 32:1–49.
20. Lane J, Ralis ZA. Changes in dimensions of large cancellous bone specimens during histological preparation as measured on slabs from human femoral heads. *Calcif Tissue Int.* 1983; 35:1–4. [PubMed: 6188519]
21. Bassett LW, Mirra JM, Cracchiolo A 3rd, Gold RH. Ischemic necrosis of the femoral head. Correlation of magnetic resonance imaging and histologic sections. *Clin Orthop Relat Res.* 1987:181–7. [PubMed: 3652573]
22. Brody AS, Strong M, Babikian G, Sweet DE, Seidel FG, Kuhn JP. John Caffey Award paper. Avascular necrosis: early MR imaging and histologic findings in a canine model. *AJR Am J Roentgenol.* 1991; 157:341–5. [PubMed: 1853819]
23. Helms, CA.; Major, NM.; Anderson, MW.; Kaplan, PA.; Dussault, R. *Musculoskeletal MRI.* 2nd. Philadelphia, PA: Saunders Elsevier; 2009.

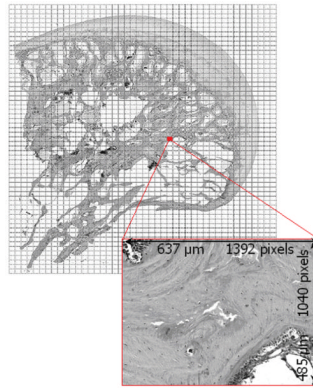


Figure 1. Reconstruction image of a femoral head section scan. Rectangular regions show the individual tissue sub-region images captured for this particular section. These high-magnification images (inset) were evaluated for osteocyte viability.

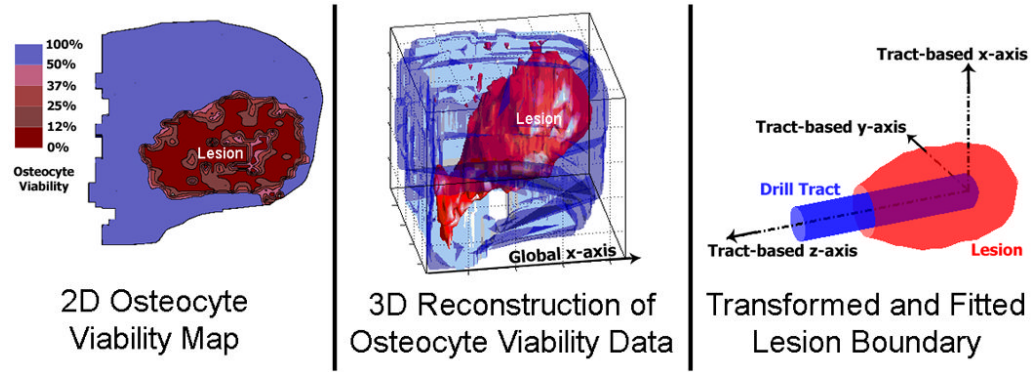


Figure 2.

Steps in the analysis of a cryoinjury-induced lesion. First, serial histology sections were evaluated for percentage of osteocyte viability in 2D (Left). Next, the fiducial markers were used to rotate and align adjacent sections for stacking in 3D (Middle). Finally, the necrotic lesion was isolated from the femoral head and transformed to a drill tract-based coordinate system. The fitted boundary was then used for lesion volume calculation (Right). The osteonecrotic lesion corresponds to the zone of <50% osteocyte viability.

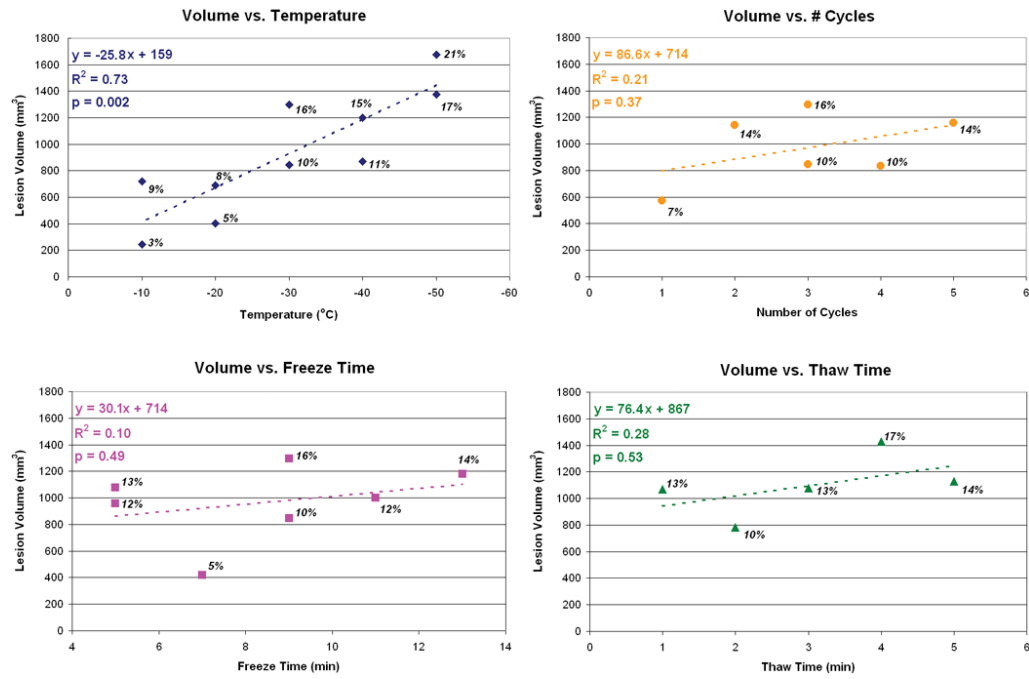


Figure 3. Effects of individual cryoinjury input parameters on necrotic lesion volumes. Each plot corresponds to one of the teaching series groups (Groups 1-4). The labels near each data point report the volume of the necrotic lesion as a percentage of the femoral head volume.

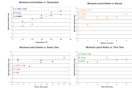


Figure 4. Effects of individual cryoinsult input parameters on maximum necrotic lesion radius. Each plot corresponds to one of the teaching groups (Groups 1-4). The overall trend in maximum lesion radius was similar to that of total lesion volume.

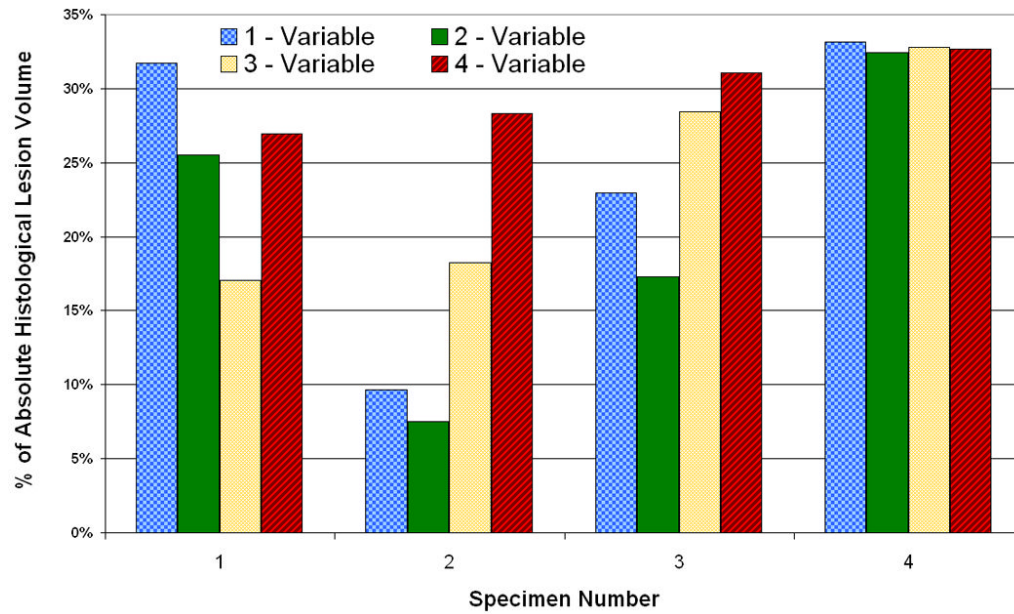


Figure 5. Errors in prediction of Group 5 lesion volume by regression models using different numbers of input variables. The one-variable model used temperature only, the two-variable model used temperature and thaw time, and the three-variable model used temperature, number of freeze/thaw repetitions, and freeze time.

Details of each cryoinsult parameter set investigated in the 4 teaching groups and the 1 testing group. A passive thaw indicated that no re-warming was applied, and the femoral head temperature was allowed to recover naturally to 30°C prior to the initiation of the next freeze cycle. Non-passive thawing involved external re-warming to 30°C using a heating wire integrated within the cryoprobe. Replicate specimens in some of the cryoinsult input parameter groups led to a total of 24 emu femoral heads comprising the teaching series (Groups 1-4).

Table 1

	Temperature	Number of Cycles	Duration of Freeze	Duration of Thaw	Animals Utilized
Baseline	-30°C	3	9 min.	passive	2
Group 1 (Temperature)	-10°C	3	9 min.	passive	2
	-20°C	3	9 min.	passive	2
	-40°C	3	9 min.	passive	2
	-50°C	3	9 min.	passive	2
	-30°C	1	9 min.	passive	1
Group 2 (Cycle Repetition)	-30°C	2	9 min.	passive	1
	-30°C	4	9 min.	passive	1
	-30°C	5	9 min.	passive	1
	-30°C	3	5 min.	passive	2
	-30°C	3	7 min.	passive	1
Group 3 (Freeze Duration)	-30°C	3	11 min.	passive	1
	-30°C	3	13 min.	passive	1
	-30°C	3	9 min.	1 min.	1
	-30°C	3	9 min.	2 min.	1
	-30°C	3	9 min.	3 min.	1
Group 4 (Thaw Duration)	-30°C	3	9 min.	4 min.	1
	-30°C	3	9 min.	5 min.	1
	-50°C	1	13 min.	passive	1
	-30°C	4	9 min.	3 min.	1
	-50°C	5	13 min.	5 min.	1
Group 5 (Testing Series)	-40°C	3	9 min.	passive	1